

Molecular Mechanism of Flip-Flop in Triple-Layer Oleic-Acid Membrane: Correlation between Oleic Acid and Water

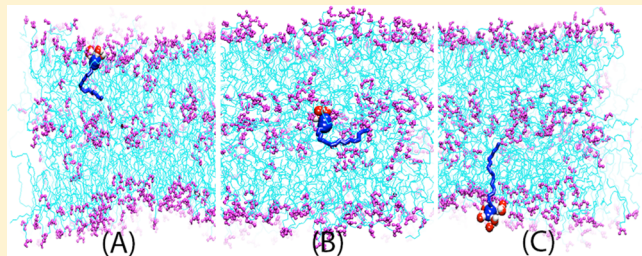
Van A. Ngo*

Department of Physics and Astronomy, University of Southern California, Los Angeles, California 90089-0242, United States

Rajiv K. Kalia, Aiichiro Nakano, and Priya Vashishta

Collaboratory for Advanced Computing and Simulations, Department of Physics and Astronomy, Department of Chemical Engineering and Materials Science, and Department of Computer Science, University of Southern California, Los Angeles, California 90089-0242, United States

ABSTRACT: We perform all-atom molecular dynamics simulations to study a pure oleic acid (OA) membrane in water that results in a triple-layer structure. We compute the pressure profiles to examine the hydrophobic and hydrophilic regions, and to estimate the surface tension ($\approx 34.5 \text{ mN/m}$), which is similar to those of lipid membranes. We observe that the membrane of OAs having a large diffusion coefficient ($0.4 \times 10^{-7} \text{ cm}^2/\text{s}$) along the normal to the membrane is an ideal model to study oleic acid flip-flop. In the model, the membrane contains a middle layer serving as an intermediate for water and OAs to easily migrate (flip-flop) from one to other leaflets. Water molecules surrounding OA head-groups help to reduce the barriers at the hydrophobic interface to trigger flip-flop events. Within 500 ns, we observe 175 flip-flop events of OAs and 305 events of water traversing the membrane. The ratio of water passing rate ($k_{\text{H}_2\text{O}} = 0.673 \text{ ns}^{-1}$) to OA flip-flop rate ($k_{\text{OA}} = 0.446 \text{ ns}^{-1}$) is 3/2. The ratio of the totally correlated water–OA events to the totally uncorrelated water–OA events, $n_{\text{cor}}/n_{\text{uncor}}$, is also 3/2. The probability of the totally and partially correlated events is 69%. The results indicate that the trans-membrane movement of water and OAs is cooperative and correlated, and agrees with experimentally measured absorption rates. They support the idea that OA flip-flop is more favorable than transport by means of functional proteins. This study might provide further insight into how primitive cell membranes work, and how the interplay and correlation between water and fatty acids may occur.



I. INTRODUCTION

Oleic acid is one of the common fatty acids that are very important in biological processes. Fatty acids not only are involved in lipid metabolism for cells¹ but also play an essential role in mediating stress² by trans-membrane movement. The trans-membrane movement of fatty acids without protein transporters is called flip-flop when they migrate from one leaflet into the other leaflet. Fatty acid flip-flop with rates of milliseconds^{2–9} has been considered as a mechanism for transport and stress relaxation across model membranes. Szostak and colleagues suggested that, when a membrane is under stress or locally deformed, flip-flop can facilitate the membrane remodeling.² However, there is a noticeable discrepancy between the measurable flip-flop rates and fast absorption rates of fatty acid monomers on lipid bilayers. For example, the absorption rate of palmitic acid to phosphatidylcholine small unilamellar vesicles is 0.024 ns^{-1} , which is at least 1000 times faster than the flip-flop rates, and almost the same for many fatty acid monomers.^{3,10,11} The absorption and transmembrane movement (by either flip-flop or functional proteins) rates should not be discrepant to ensure the equilibrium of fatty acid transport through cellular membranes, which is described by three distinct processes:

absorption, trans-membrane movement, and desorption. The discrepancy, however, lies in difficulties of tracking and measuring flip-flop events.

It is elusive to directly observe and analyze flip-flop events.^{3,6,12} In advanced fluorescence techniques,^{2,9} one first attaches fluorescence molecules to fatty acids and then measures flip-flop rates from the decay of the fluorescence response. The fluorescence techniques are subjected to a time-limited resolution with an order of microseconds. They currently have not been able to identify any flip-flop events occurring in a few hundred nanoseconds. The techniques usually provide upper bounds to flip-flop rates. Moreover, the weight of fluorescence molecules might have some effects on the accuracy of the measurements.⁹ An accurate technique should be able to capture the lowest flip-flop rates. The accuracy of the lowest rates is critically essential because it provides direct evidence for whether the trans-membrane movement by flip-flop is more favorable for cellular membranes than the transport movement by functional proteins.^{5,6,12–15}

Received: July 20, 2012

Revised: September 20, 2012

Published: October 17, 2012



While the submicrosecond time-scale to measure the lowest rates has been a challenge, it is achievable in molecular dynamics (MD) simulations. In MD simulations, one can easily identify and analyze the movement of fatty acids across membranes. Although there are MD simulations aimed to investigate the effects of fatty acids on lipid-membrane properties,^{16,17} no all-atom MD simulation has been carried out to study the structure, or particularly remodeling of pure oleic acid (OA) membranes. Notman et al.¹⁷ used a coarse-grained model to study the structures of pure OA membranes but did not report a flip-flop mechanism of coarse-grained OAs in membrane remodeling. Gurtovenko et al.¹⁸ examined the correlation between a transient water pore and the molecular flip-flop mechanism of lipid molecules under applied electric fields. They concluded that water molecules instantaneously passing through a lipid membrane promote the flip-flop of lipid molecules. However, the same correlation between the passage of water and flip-flop in pure OA membranes has not been identified. It might suggest a simple molecular mechanism for the membrane remodeling.

In this paper, we perform all-atom MD simulations to study the remodeling of a pure OA membrane from a crystalline structure, and investigate the molecular mechanism of flip-flop events. Our resulting OA membrane has a thickness of 46 Å and three layers of hydrophilic COOH head-groups. We measure the pressure profiles to examine the favorable and unfavorable interactions of OAs with water in the membrane, and to compute the surface tension. We observe that the middle layer exists as an intermediate for fast rearrangement of OAs. Every flip-flopping OA molecule stays most of the time in the middle layer before migrating into the others. We also observe fast passage of water molecules across the membrane (called water events). We hypothesize that the movement of water molecules cooperatively enhances the flip-flop of OAs. We quantify the cooperative movement by counting water events triggering OA flip-flop events. The rates of OA flip-flop and water events are $k_{\text{OA}} = 0.446 \text{ ns}^{-1}$ and $k_{\text{H}_2\text{O}} = 0.673 \text{ ns}^{-1}$, which are in better agreement with the absorption rates of fatty acid monomers ($\approx 0.024 \text{ ns}^{-1}$) on lipid vesicles³ than the measurable values of flip-flop rates ($\sim \text{ms}^{-1}$) in experiments.

II. METHOD

We prepared a bilayer of oleic acid (OA) molecules (Figure 1A). The initial structure of the bilayer is in the crystalline γ -phase.^{19,20} The density of the crystal membrane is 0.89 g/cm³. Each of the top and bottom layers has 441 OAs (Figure 1A). The membrane is then sandwiched by TIP3P water facing the hydrophilic carboxyl groups COOH. The initial dimensions of the system are $10 \times 10 \times 10 \text{ nm}^3$. The total number of atoms is 95 832. Charmm27 force-fields^{21,22} for TIP3P water and OA were used. The force-field parameters of hydrocarbon chains of dioleoyl-glycero-phosphocholine (DOPC) lipid were applied to OA's hydrocarbon chain, since they are the same. In Charmm27, since the force-field parameters for COOH of protonated aspartic and glutamic acids based on acetic acid (CH_3COOH) are indistinguishable, it is reasonable to apply these force-field parameters to the COOH of OA. There is no net charge in the system.

The molecular dynamics (MD) simulations were implemented by the NAMD package.²³ First, we used a conjugate gradient for 10 000 steps to remove any high-energetic contacts in the system; then, we performed simulations using NVT with Langevin dynamics for 10 ns, and NPT with constant area (NPAT) in the xy -plane to relax the crystalline OA membrane at $T = 323 \text{ K}$ for

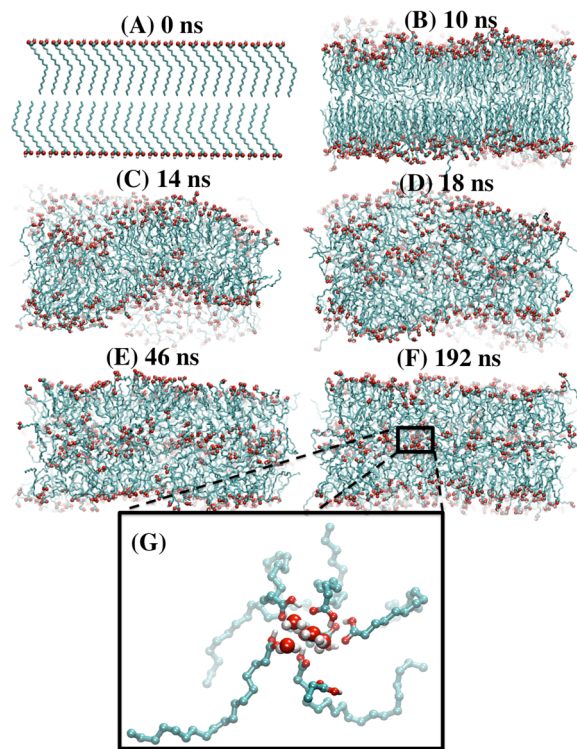


Figure 1. Snapshots of the oleic acid (OA) membrane during simulations. (A) Initial crystalline membrane in the γ -phase. (B) OA bilayer in NVT. (C–E) OA membrane in NPAT. (F) OA membrane in isotropic NPT. Red, white, and cyan colors are oxygen, hydrogen, and carbon atoms, respectively. Water is not shown. (G) Four water molecules surrounded by OAs. Hydrogen atoms bonded to carbon atoms are not shown.

36 ns. The damping coefficient for Langevin dynamics was 5 ps⁻¹. The time step was 1 fs for NVT and 2 fs for pressure coupling. The system was coupled with isotropic NPT for production runs. (Constant area was turned off.) The target pressure was set to 1 bar. The barostat oscillation time and barostat damping time were 200 and 100 fs, respectively. The particle mesh Ewald method was used to compute Coulomb interaction with a grid size of about 1 Å. The cutoff for nonbonded interactions was 12 Å. All nonbonded interactions were smoothed at 10 Å. The exclusion 1–4 interaction was turned on with the scaling being 0.833 33. The trajectories were saved every 10 ps for analysis. The total production time was 500 ns. The final dimensions are $10.1 \times 10.1 \times 94.9 \text{ nm}^3$. The figures were rendered by VMD.²⁴

We adopted the method of computing pressure profiles developed by Lindahl et al.²⁵ and the Schulten group.²⁶ The local pressure tensor $P_{\alpha\beta}(z)$ within a given slab centered at z is

$$P_{\alpha\beta}(z) = \frac{1}{\Delta V} \left[\sum_i m_i \vec{v}_i \otimes \vec{v}_i - \sum_{i < j} \vec{F}_{ij} \otimes \vec{r}_{ij} \right] \quad (1)$$

where $\alpha \equiv (x, y, z)$, $\beta \equiv (x, y, z)$, ΔV is the slab's volume, and the sums are run over the particles in the slab. The stress profile $\pi(z)$ is defined as $[P_{xx}(z) + P_{yy}(z)]/2 - P_{zz}(z)$. The surface tension is computed as $\gamma = \int_{-0.5L_z}^{0.5L_z} \pi(z) dz$, where L_z is the z -dimension normal to the OA membrane. In our simulation, we divided the z -dimension into 94 slabs to compute the diagonal pressures $P_{\alpha\alpha}(z)$, which are convergent within 335 ns (=335 000 frames).

To observe OA flip-flops, the C1 atom of COOH having z_{C1} with respect to the center-of-mass of the membrane is chosen

to detect the starting (t_{start}) and finishing (t_{finish}) time of a flip-flop event. When z_{C1} is either $<22 \text{ \AA}$ or $>-22 \text{ \AA}$, t_{start} is marked. When z_{C1} becomes either $<-22 \text{ \AA}$ or $>22 \text{ \AA}$, t_{finish} is recorded. A complete flip-flop event of OA is accounted if $t_{\text{start}} < t_{\text{finish}}$. Flip-flop duration τ is computed as $t_{\text{finish}} - t_{\text{start}}$.

To observe water traversing the OA membrane, the z -coordinate of the oxygen atom of water (z_{OW}) with respect to the center-of-mass of the membrane is used to detect the starting (t_{start}) and finishing time (t_{finish}) of a water event. When z_{OW} is either $<22 \text{ \AA}$ or $>-22 \text{ \AA}$, t_{start} is marked. When z_{OW} becomes either $<-22 \text{ \AA}$ or $>22 \text{ \AA}$, t_{finish} is recorded. A complete event of water is counted if $t_{\text{start}} < t_{\text{middle}} < t_{\text{finish}}$, where t_{middle} is the time when a water molecule passes the middle region ($-5 \text{ \AA} < z_{\text{OW}} < 5 \text{ \AA}$). The time for a water molecule traversing the membrane is $t_{\text{finish}} - t_{\text{start}}$.

III. RESULTS AND DISCUSSION

Triple-Layer Structure. First, we describe the remodeling of the initial crystalline bilayer (Figure 1A) to triple-layer structures (Figure 1E–F). Figure 1B shows the oleic acid (OA) bilayer after 10 ns of thermalization with NVT. This bilayer is significantly disordered during 8 ns when pressure coupling (NPAT) was turned on (Figure 1C,D). At the end of this coupling (Figure 1E), the disordered distribution of OAs remodels into a triple-layer structure. The remodeling after being disordered somewhat resembles the rearrangements after being perturbed in pure fatty acid membranes in experiments.² At this point, one can continuously use NPAT for the rest of the simulations; however, the availability of area per OA is unknown for keeping the area fixed. Thus, we used NPT for the rest of the simulations to let the system adjust in all directions. Using isotropic NPT, the area and triple-layer structure remain almost the same (Figure 1F). At the middle of this membrane, we frequently observe that few water molecules can migrate from both sides and attract OAs, as seen in Figure 1G. This suggests some interesting properties of this membrane, but before analyzing, we shall provide some arguments for the triple-layer structure.

Although there is no experimental evidence for the triple-layer structure, let us argue that there is a possibility of the triple-layer OA membrane due to the presence of water. We are not concerned with how the initial bilayer membrane is perturbed but whether an equilibrium structure of OAs in water can be reached.²⁷ It is noted that without water the crystalline γ -phase has only carboxyl ($-\text{COOH}$) groups forming hydrogen bonds along the normal between two layers in a unit cell.^{19,20} This structure exists below $-2.2 \text{ }^\circ\text{C}$, and above $16 \text{ }^\circ\text{C}$ irreversibly transforms into the crystalline β -phase, whose surface structure consists of both methyl ($-\text{CH}_2$) and carboxyl groups in two layers in a unit cell. This transformation indicates that OAs flip 180° in one layer even without water. Accordingly at $50 \text{ }^\circ\text{C}$ with water, OAs can move drastically in each layer and between the only two layers in Figure 1A–D. Szostak and colleagues observed that such drastic movements like flip-flop help relaxing stress and remodeling in fatty acid membranes.^{2,28} In addition, the length of OA is shorter than a dioleoyl-glycero-phosphocholine (DOPC) lipid, which is composed of a dipolar hydrophilic headgroup and two hydrocarbon chains with the same length as OA. These hydrocarbon chains form the water-excluded region in lipid bilayers, which is also observed in the OA membrane (see Figure 2).

The weight of the dipolar hydrophilic head-groups on the surface of lipid bilayers is heavier than that of COOH. The lighter COOH with the hydrocarbon chain can diffuse much faster than the dipolar ones, and can be strongly influenced by the

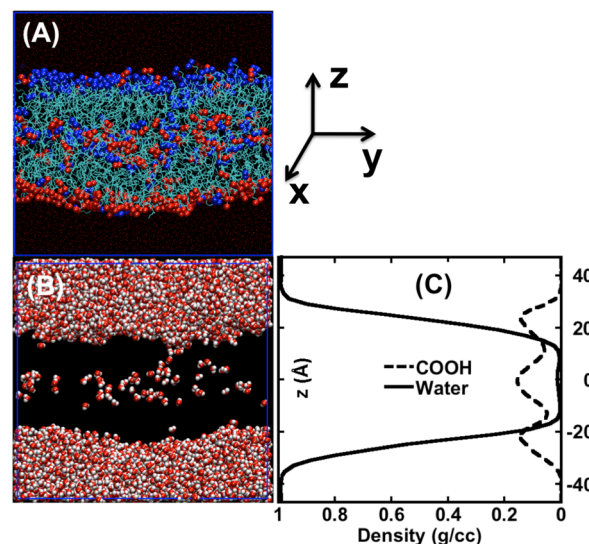


Figure 2. (A) Snapshot of the OA membrane during simulations. Red (initially at the bottom) and blue (initially at the top) spheres are COOH head-groups. Cyan lines are carbon chains. (B) Snapshot of water in the system. Red and white spheres are oxygen and hydrogen atoms, respectively. (C) Density of water and COOH along the z -direction with a bin width of 2 \AA . The data are averaged over 500 ns.

diffusion of water (will be discussed). Consequently, the bilayer structure (Figure 1A,B) of OAs with water at $50 \text{ }^\circ\text{C}$ and 1 bar is unstable, and ultimately transforms into the triple-layer structure (Figure 1F). Moreover, the force-field parameters of hydrocarbon chains of DOPC and of protonated aspartic or glutamic acid have been well tested; thus, the combination for OAs is reasonable.²⁹ We shall examine the triple-layer structure, and compare with the bilayer structure of lipids to show that this triple-layer structure is physically stable.

Now, we investigate how OA and water molecules distribute in the membrane. Figure 2A shows a snapshot of the membrane evolving from the crystalline structure in Figure 1A. Initially, OAs are at either the top (COOH colored in blue) or bottom (COOH colored in red) layers. During thermalization, OAs form the middle layer and migrate across the membrane, and little water exists at the middle of the membrane (Figure 2B). To characterize the triple-layer structure, we measure water and COOH densities. We observe that the water and COOH densities averaged over 500 ns in NPT are not largely different from those averaged over the last 13.5 ns in NPAT. In Figure 2C, the equilibrium density of water reduces from 0.989 g/cm^3 from $|z| \approx 38 \text{ \AA}$ to $|z| \approx 10 \text{ \AA}$. It is 0.012 g/cm^3 at the middle, while it was about 0.02 g/cm^3 during NPAT. The reduction from 0.02 to 0.012 g/cm^3 means that several water molecules in the middle were pushed out the middle during the further thermalization process (NPT). In the COOH density plot, the three peaks have the same order of magnitude ($\approx 0.15 \text{ g/cm}^3$), which does not noticeably deviate from the values, 0.154 – 0.168 g/cm^3 , during the last 13.5 ns in NPAT. These results suggest that thermalization with NPAT, which is usually used for simulating membranes, indeed induces the triple-layer structure. Without a reliable area per OA, the NPT thermalization was then performed.

The symmetric distribution of the COOH density confirms that the membrane is in equilibrium. On the basis of the minima of the COOH density, we define that OAs belong to either the top or bottom leaflet if the z -coordinates of carbon atoms of

COOH head-groups with respect to the center-of-mass of the membrane are either greater than 12 Å or less than -12 Å, respectively. The averaged positions of COOH in the top and bottom leaflets along the z-direction are at $z = \pm 23$ Å. The thickness is thus 46 Å, whereas the thickness of the initial crystalline membrane is 42 Å. On average, there are 257 OAs in each of the top and bottom leaflets. Thus, the area per OA in the leaflets is 39.7 Å^2 . The middle layer contains the rest, 368 OAs or 41.7% of all the OAs.

The thickness of the OA membrane, ≈ 46 Å, is in a range from 32.8 to 48 Å of lipid bilayers.²⁶ Since the area per lipid is typically about 64 Å^2 ,³⁰ and each lipid has two hydrocarbon chains, the area per hydrocarbon chain in lipid bilayers is 32 Å^2 , which is about 8 Å^2 smaller than the area per OA, 39.7 Å^2 . If taking into account the size of dipolar lipid head-groups, which is larger than that of COOH, the area per OA is consistently larger than that per hydrocarbon chain in lipid bilayers.

The membrane has a small level of hydrophobicity. The level of hydrophobicity can be inferred from the low water density ($c_{\text{H}_2\text{O}}(z=0) = 0.012 \text{ g/cm}^3$) at the middle of the membrane (see Figure 2C). From the water-density profile, we estimate the potential of mean force,³¹ which is computed by $-RT \ln[c_{\text{H}_2\text{O}}(0)/c_{\text{H}_2\text{O}}] = 1.97 \text{ kJ/mol}$, where R is the gas constant, T is 323 K, and $c_{\text{H}_2\text{O}} = 0.989 \text{ g/cm}^3$ is the bulk density of water outside the membrane. The potential of mean force indicates the free-energy barrier for water to permeate the OA membrane. It is about 13.5 times smaller than the free-energy barrier for water to permeate lipid bilayers ($\approx 26 \text{ kJ/mol}$) at $T = 350 \text{ K}$.³¹

To further demonstrate the properties of the OA membrane, we measure the mean square displacements (MSD) in the lateral xy -plane and along the normal to the membrane (see Figure 3).

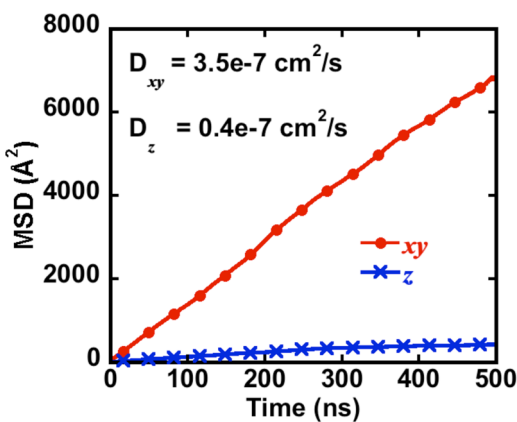


Figure 3. Mean square displacements (MSDs) of OAs in the xy -plane and z -normal to the membrane. The positions of carbon atoms of COOH head-groups are used to compute the MSDs.

From the slope of the MSD in the xy -plane, the lateral self-diffusion coefficient is $3.5 \times 10^{-7} \text{ cm}^2/\text{s}$, which is about 9 times higher than the experimental self-diffusion coefficient³² ($\approx 0.45 \times 10^{-7} \text{ cm}^2/\text{s}$) of dimyristoyl-phosphatidyl-choline (DMPC) lipid molecules at 26 °C. The DMPC lipid has two little shorter carbon chains but a heavier headgroup than OA. Thus, due to the larger masses,³³ the self-diffusion coefficient of DMPC lipids is consistently 9 times smaller than that of OA. In addition, the diffusion coefficient along the normal direction to the membrane, $D_z = 0.4 \times 10^{-7} \text{ cm}^2/\text{s}$, is at least 2 orders of magnitude higher than that of lipid molecules ($\sim 10^{-9} \text{ cm}^2/\text{s}$). This diffusion

coefficient suggests that the OA membrane is ideal in simulation time-scales to investigate the trans-membrane movement from one (top or bottom) leaflet to the other (bottom or top) leaflet, which is defined as flip-flop.

To compare the mechanical properties of the OA membrane with those of lipid membranes, we examine the pressure profiles (see section II). Pressure profiles have been used to describe structures of lipid membranes in gel and liquid phases.^{26,34} The structures, favorable and unfavorable interactions, are reflected from the modulations, the positive and negative peaks of pressure profiles. The pressure profiles of the OA membrane (see Figure 4) are smaller in magnitude than those of liquid-

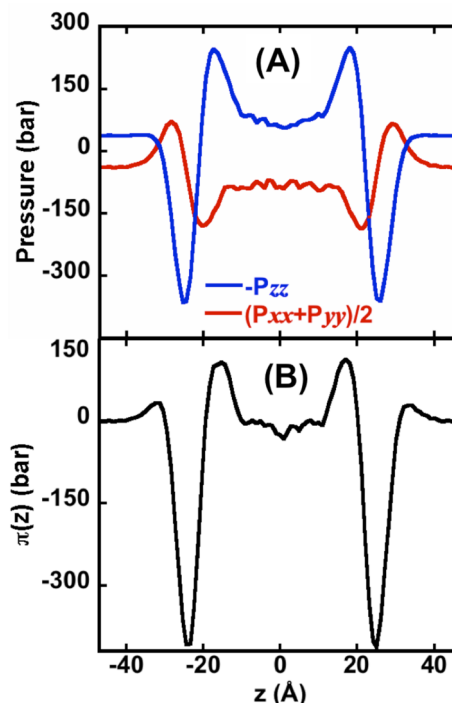


Figure 4. (A) Lateral pressure $(P_{xx} + P_{yy})/2$ and normal pressure $-P_{zz}$. (B) Stress profile $\pi(z) = (P_{xx} + P_{yy})/2 - P_{zz}$ along the z -direction normal to the membrane with a bin width of 1 Å.

disordered lipid membranes³⁴ (L_a) but still preserve the hydrophilic and hydrophobic interfaces of a model membrane. In a direction into a membrane, a hydrophilic or hydrophobic interface is defined as a region where $\pi(z)$ goes from positive to negative or from negative to positive, respectively. Near the hydrophilic interfaces, the small positive peaks of $\pi(z) = 30 \pm 3$ bar at $z \approx \pm 33$ Å (Figure 4B) are mainly due to the lateral pressure $(P_{xx} + P_{yy})/2$ (Figure 4A). These peaks are significantly smaller than those of L_a which are about 800 bar. The negative peaks ($= -405 \pm 5$ bar) of $\pi(z)$ at $z \approx \pm 23$ Å near the hydrophobic interfaces indicate that the membrane is not as compressive as L_a . These small negative peaks are consistent with the large diffusion. Interestingly, at $z \approx \pm 17.5$, $\pi(z)$ is 100 ± 10 bar due to the normal pressure $-P_{zz}$, that is larger than the first two positive peaks. On the contrary, the first two positive peaks of $\pi(z)$ of L_a are the largest. There is also a small negative peak near $z = 0$, which indicates slight compression. The peak can be attributed to the presence of water molecules around $z = 0$, as shown in Figure 1G. Water molecules attract several COOH head-groups, which make the middle layer slightly compressive. The zero values of the stress profile between $z = -10$

and 10 Å indicate that OA and water molecules are also freely diffusive. Those properties of $\pi(z)$ suggest that water molecules can diffuse more easily into the membrane than lipid bilayers. The resulting surface tension $\gamma(OA)$, the area under $-\pi(z)$, is 34.5 mN/m, which falls in a range for those of simulated and experimental lipid bilayers, e.g., $\gamma(POPC) = 35.7$ mN/m at 70.56 Å²/lipid.^{26,35,36}

Oleic Acid Flip-Flopping and Water Traversing Membrane. The main purpose of this paper is to suggest a strong correlation between oleic acid (OA) flip-flop and the transmembrane movement of water. We find that there are 175 flip-flop events of OAs in 500 ns. Figure 5A shows the histo-

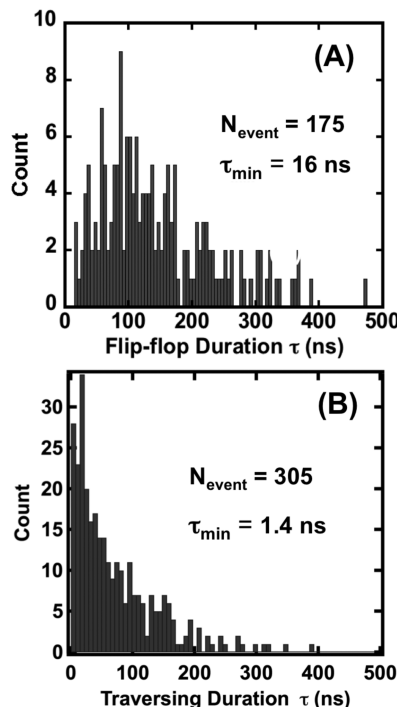


Figure 5. Histograms of flip-flop (A) and traversing (B) durations of OAs and water, respectively.

gram of the flip-flop events, where τ denotes flip-flop duration. The shortest duration τ_{\min} is 16 ns. 65% of the events have τ between 50 and 200 ns. Figure 5B shows the histogram of the water events, whose τ is also the duration for water molecules to traverse the membrane. We find that 305 events of water molecules finish the migration in 500 ns. The shortest duration τ_{\min} is about 1.4 ns. 75% of events have τ less than 100 ns. As a result, water can move much faster than OA across the membrane.

To measure the rates for water and OA flip-flop events, we plot the accumulated numbers (NE_{H_2O} and NE_{OA}) of both events over simulation time (t_{finish}) in Figure 6. Linearly fitting those numbers as functions of time, we find that $NE_{H_2O} \sim 0.673t$ and $NE_{OA} \sim 0.446t$. The slopes are the rates (k) of the events. The rates of water and OA flip-flop events are $k_{H_2O} = 0.673$ ns⁻¹ and $k_{OA} = 0.446$ ns⁻¹. The ratio, $k_{H_2O}/k_{OA} = 3/2$, means that on average there are 3 waters and 2 OAs, which finish migrating from one to the other side of the membrane. The trans-membrane movement of water has a very high rate, $k_{H_2O} = 0.673$ ns⁻¹. The rates of water and OA flip-flop events are in the order of the water-permeation rate in bacterial-glycol facilitator proteins³⁷ (~0.5 ns⁻¹). They are about 6 times

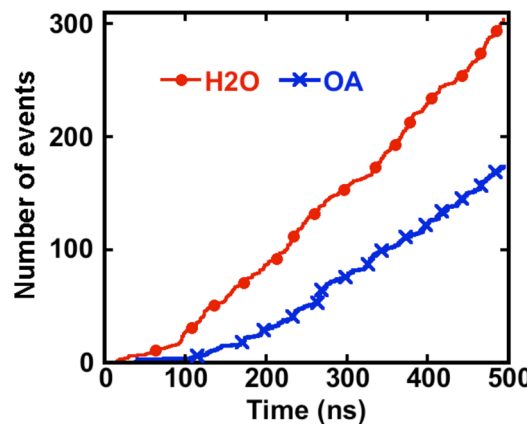


Figure 6. Accumulated numbers (NE) of water and OA molecules completely migrating across the membrane versus time (t_{finish}) (see section II).

slower than the water-permeation rate in aquaporin-1 proteins³⁸ (~3.0 ns⁻¹), which have a special water-selectivity function.³⁹ The water-selectivity function is composed of asparagine, proline, and alanine, each of which also possesses a COOH headgroup similar to that of oleic acid. The similarity supports the hypothesis that the migrations of water and oleic acid are correlated.

Figure 7 shows how OA and water molecules migrate across the membrane. These two molecules start moving into the

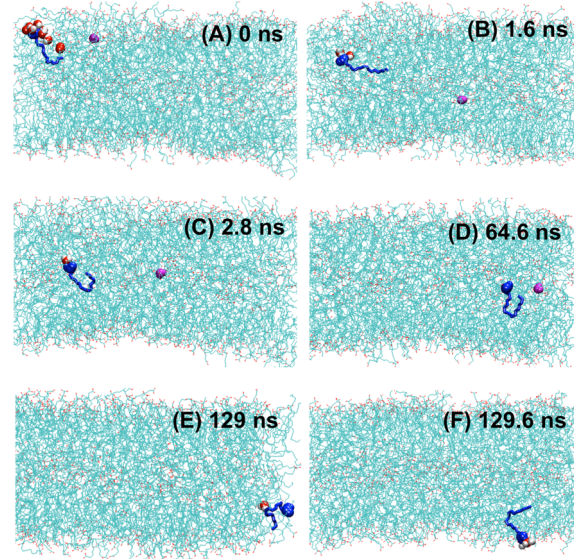


Figure 7. Snapshots of OA flip-flopping and water-traversing events. The flip-flopping molecule is highlighted in blue. Its headgroup and tail are denoted by balls and sticks, respectively. The surrounding water molecules of the headgroup are found within a search of 3.5 Å. The traversing water molecule is highlighted in magenta. Red, cyan, and white are oxygen, carbon, and hydrogen atoms, respectively. The starting time for these events is 71.4 ns. The numbers denote the durations after the starting time.

membrane at about 71.4 ns (Figure 7A), which denotes the starting time, t_{start} (see section II), and finish the migration in almost the same duration, $\tau \approx 129$ –130 ns. Initially, the OA is surrounded by a few water molecules within 3.5 Å from the COOH headgroup. The traversing water molecule is quite

close to the OA. After only 1.6 ns (Figure 7B), the water molecule reaches the middle of the membrane, and the OA goes about a quarter of the membrane thickness. These molecules are then fluctuating around the middle layer for a very long time (~ 100 ns). The COOH headgroup is sometimes hydrated and dehydrated, and moves close to the traversing water molecule (Figure 7C,D). It can both make hydrogen bonds with other OAs and with water, which explain the change in the hydration level. Finally, at 129 ns, the water molecule completely migrates to the other side (Figure 7E), and the OA delays the migration for 0.6 ns (Figure 7F). Here, the OA does not directly drag the water molecule during migration. One reason is that the hydrogen bonds between OAs and water are not strong enough for water to hold onto the COOH headgroups. Since there are water-excluded regions in the membrane, the water molecule moves fast to the middle and vice versa (see Figure 7A,B). Water also has a smaller size than OA; on average, it takes a longer time for OA to reach and move away from the middle layer (see Figure 5). For those reasons, water and OA molecules cannot together migrate across the membrane in every step.

We observe that in many cases water molecules surrounding COOH help trigger the flip-flop events. In Figure 8, we show

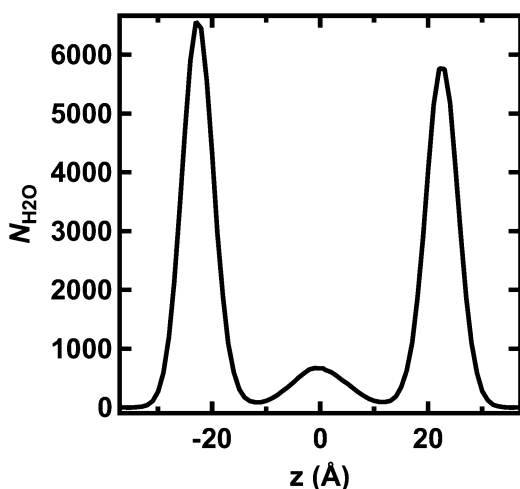


Figure 8. Averaged number of water molecules around COOH per flip-flopping OA versus z during migration. The bin width of slaps along the z -direction is 1 Å. Water molecules are counted within 3.5 Å of COOH throughout 500 ns in each slap. No OA molecule is found for $|z| > 36$ Å.

the number of water molecules, N_{H_2O} , surrounding the COOH head-groups of the flip-flopping OAs throughout 500 ns. This number is counted in every slap along the z -direction with a bin width of 1 Å, and averaged over 175 flip-flop events. While its variation indicates the relative change of hydration level of COOH across the membrane, its zero value implies no OA located at $|z| > 36$ Å and no neighboring water molecules. Since there are few water molecules at the middle, the peak of N_{H_2O} is significantly smaller than the others. Although the other two peaks at $z = \pm 22.5$ Å are not the same, they simply imply the different residing times of flip-flopping OAs when starting and finishing migration. Thus, these two peaks indicate almost the same and highest hydration level near the hydrophobic interfaces (see Figure 4B). The large values of N_{H_2O} at $|z| < 22.5$ Å suggests that some water molecules accompany the OAs

into the interfaces. Importantly, the nonzero minimum values of N_{H_2O} , ≈ 90 , at $z = \pm 12$ Å indicate that the flip-flopping OAs always contact with water molecules several times, as already seen in Figure 7C. As a result, these water molecules help to reduce barriers at the hydrophobic interfaces.

To further quantitatively correlate the 305 water events and the 175 OA flip-flop events, we analyze their starting time t_{start} (see section II), regardless of migration directions. We divide the 500 ns simulation time into 100 bins. WA(i) and OA(i) store the number of the events in the i th bin. Here, index i is $\text{floor}(t_{\text{start}}/5)$ plus 1, which returns an integer. For example, there are 11 waters and 5 OA events in the third bin, which start migrating between 10 and 15 ns. We define water and OA events as totally correlated if $[\text{WA}(i) - \text{WA}(i - 1)] \times [\text{OA}(i) - \text{OA}(i - 1)] > 0$, partially correlated if $[\text{WA}(i) - \text{WA}(i - 1)] \times [\text{OA}(i) - \text{OA}(i - 1)] = 0$ and $\text{WA}(i) \geq \text{OA}(i) > 0$, and uncorrelated if $[\text{WA}(i) - \text{WA}(i - 1)] \times [\text{OA}(i) - \text{OA}(i - 1)] < 0$. We find 33 bins (n_{cor}) having totally correlated events, 16 bins having partially correlated events, and 22 bins (n_{uncor}) having uncorrelated events. The totally correlated events mean that, as a number of water events increases or decreases, so does a number of flip-flop events within an observation interval. In contrast to the totally correlated events, the uncorrelated ones mean that water has no effect on OA flip-flop. The probability of the correlated events is $(33 + 16)/71 = 69\%$. A probability greater than 50% indicates that the trans-membrane movements of water and OA are likely cooperative. (If the probability is less than 50%, it means that the events of water and OA are totally random.) The ratio of the totally correlated to uncorrelated events is $n_{\text{cor}}/n_{\text{uncor}} = 3/2$. It indicates that, in every 5 events, there are 3 water events totally correlated with flip-flop events. This ratio $n_{\text{cor}}/n_{\text{uncor}}$ coincides with k_{H_2O}/k_{OA} . This coincidence confirms the quantitative analysis of the correlation.

In comparison with the lipid flip-flop mechanism, which is a pore-mediated process,^{18,40} our findings bear some similarities and differences. In the lipid mechanism, the migration of lipid molecules across bilayers occurs simultaneously with the formation of transient water pores. Due to the formation, lipid molecules around the pores rearrange to facilitate equilibrium processes and mediate stress. The stress mediation is also found in experiments by Szostak's group on fatty acid membranes.² In our oleic acid membrane, water molecules also help triggering and correlate with the flip-flop events of OAs, however, not as directly as in the lipid flip-flop mechanism, since there is no transient water pore. Once a transient pore appears, a lipid flip-flops within 10 ns, which is about the order of the minimum flip-flopping time of OAs, $\tau_{\min} = 16$ ns. Most of the flip-flop times are about 100 ns because OAs can reside in the intermediate middle layer, which can facilitate the migration of both water and OAs without the need of transient water pores like in lipid bilayers.

This correlation between the rates of water and flip-flop events might be the simplest mechanism for fatty acid transports. Now in what cases or membranes can this mechanism take place? First, Szostak and colleagues showed the existence of fatty acid (including oleic acid) membranes, which was thought to be the primitive membranes.^{2,28} Second, many researchers^{20,41,42} observed the crystalline structures of oleic acid without water, whose unit cells have two layers of oleic acids. However, the evidence of the bilayer structures does not rule out the possibility of the triple-layer structure. Third, it should be noted that our triple-layer structure was thermally remodeled from the

γ -phase crystalline structure, which exists below -2°C . With the presence of water at 50°C , the favorable interactions between the COOH head-groups and water and the unfavorable interactions between the aliphatic chains and water always result in a water-excluded region. Such a water-excluded region in the OA membrane with the same thickness as lipid membranes is unlikely to have the bilayer structure, since the length of OAs is not as long as those of lipids, and COOH is not as heavy as dipolar lipid head-groups. It is noted that the area per OA, 39.7 \AA^2 in the top and bottom leaflets, is consistent with the area per hydrocarbon chains in several bilayers³⁰ ($\sim 32\text{ \AA}^2$), and the surface tension, 34.5 mN/m , is about the same as those of simulated and experimental lipid bilayers.^{26,35,36} These results suggest that it is possible for pure OA triple-layers to exist within lipid bilayers without changing the elasticity of lipid membranes.

Finally, the flip-flop rate is only 20 times faster than absorption rates ($\approx 0.024\text{ ns}^{-1}$) of fatty acid monomers on lipid vesicles in experiments.^{3,10,11} Note that this absorption rate is almost the same for many fatty acid monomers. It is many orders of magnitude faster than the experimentally measurable values of flip-flop rates ($\sim \text{ms}^{-1}$). In any cases, one would expect that the transmembrane movement by either flip-flop or proteins and absorption rates of fatty acids should not be widely different. Accordingly, the flip-flop mechanism is more favorable than transport proteins but is currently not well supported by the direct experimental data, i.e., accurate flip-flop rates close to 0.024 ns^{-1} . If the absorption rates are truly extremely faster than the transport rates, there is a possibility that many OAs fast absorbed on lipid surfaces can form a separated aggregate probably having the triple-layer structure. As shown in our simulations, this triple-layer structure suggests an enhancement in the transport rate without the need of transport proteins. As a result, the triple-layer structure is probably critical for an extremely fast transport mechanism in general cellular membranes.

IV. CONCLUSIONS

We have simulated a pure oleic acid (OA) membrane in water that consists of three layers. The triple-layer structure also has pressure profiles somewhat similar to those of lipid membranes. The surface tension, 34.5 mN/m , is in a range for those of lipid membranes. It suggests a possible existence of separated pure OA aggregates in lipid membranes. We observed that (i) several water molecules surrounding COOH head-groups help to reduce the barriers at the hydrophobic interfaces to trigger flip-flop events, and (ii) the middle layer serves as an intermediate for water and OAs to migrate from one side to the other side of the membrane (defined as flip-flop). Within 500 ns , there are 175 flip-flop events of OAs and 305 events of water traversing the membrane. The ratio of water-traversing rate ($k_{\text{H}_2\text{O}} = 0.673\text{ ns}^{-1}$) to OA flip-flop rate ($k_{\text{OA}} = 0.446\text{ ns}^{-1}$) is $3/2$. The ratio of the totally correlated water–OA events to the totally uncorrelated water–OA events, $n_{\text{cor}}/n_{\text{uncor}}$, is also $3/2$. The probability of having the partially and totally correlated events is 69%. The results indicate that the trans-membrane movement of water and OAs is cooperative and correlated, and agrees with the experimentally measured absorption rate, 0.024 ns^{-1} . They support the idea that OA flip-flop is more favorable than transport by means of functional proteins. This study might provide further insight into how primitive cell membranes work, and how the interplay and correlation between water and fatty acids may occur.

AUTHOR INFORMATION

Notes

The authors declare no competing financial interest.

ACKNOWLEDGMENTS

We thank the referees for useful comments and suggestions. We acknowledge DOE and NSF for financial support.

REFERENCES

- (1) Mashek, D. G.; Coleman, R. A. *Curr. Opin. Lipidol.* **2006**, *17*, 274–278.
- (2) Bruckner, R. J.; Mansy, S. S.; Ricardo, A.; Mahadevan, L.; Szostak, J. W. *Biophys. J.* **2009**, *97*, 3113–3122.
- (3) Hamilton, J. A. *J. Lipid Res.* **1998**, *39*, 467–481.
- (4) Hamilton, J. A. *Curr. Opin. Lipidol.* **2003**, *14*.
- (5) Hamilton, J.; Brunaldi, K. *J. Mol. Neurosci.* **2007**, *33*, 12–17.
- (6) Hamilton, J. A.; Kamp, F. *Diabetes* **1999**, *48*, 2255–2269.
- (7) Kamp, F.; Hamilton, J. A. *Prostaglandins, Leukotrienes, and Fatty Acids* **2006**, *75*, 149–159.
- (8) Kamp, F.; Zakim, D.; Zhang, F.; Noy, N.; Hamilton, J. A. *Biochemistry* **1995**, *34*, 11928–11937.
- (9) Simard, J. R.; Pillai, B. K.; Hamilton, J. A. *Biochemistry* **2008**, *47*, 9081–9089.
- (10) Noy, N.; Zakim, D. *Biochemistry* **1985**, *24*, 3521–3525.
- (11) Daniels, C.; Noy, N.; Zakim, D. *Biochemistry* **1985**, *24*, 3286–3292.
- (12) Kampf, J. P.; Cupp, D.; Kleinfeld, A. M. *J. Biol. Chem.* **2006**, *281*, 21566–21574.
- (13) Hamilton, J.; Johnson, R.; Corkey, B.; Kamp, F. *J. Mol. Neurosci.* **2001**, *16*, 99–108.
- (14) Hirsch, D.; Stahl, A.; Lodish, H. F. *Proc. Natl. Acad. Sci. U.S.A.* **1998**, *95*, 8625–8629.
- (15) Kleinfeld, A. M. *J. Membr. Biol.* **2000**, *175*, 79–86.
- (16) Huber, T.; Rajamoothi, K.; Kurze, V. F.; Beyer, K.; Brown, M. F. *J. Am. Chem. Soc.* **2001**, *124*, 298–309.
- (17) Notman, R.; Noro, M. G.; Anwar, J. *J. Phys. Chem. B* **2007**, *111*, 12748–12755.
- (18) Gurtovenko, A. A.; Vattulainen, I. *J. Phys. Chem. B* **2007**, *111*, 13554–13559.
- (19) Kaneko, F.; Yamazaki, K.; Kitagawa, K.; Kikyo, T.; Kobayashi, M.; Kitagawa, Y.; Matsuura, Y.; Sato, K.; Suzuki, M. *J. Phys. Chem. B* **1997**, *101*, 1803–1809.
- (20) Suzuki, M.; Ogaki, T.; Sato, K. *J. Am. Oil Chem. Soc.* **1985**, *62*, 1600–1604.
- (21) Pitman, M. C.; Suits, F.; MacKerell, A. D.; Feller, S. E. *Biochemistry* **2004**, *43*, 15318–15328.
- (22) Feller, S. E.; Gawrisch, K.; MacKerell, A. D. *J. Am. Chem. Soc.* **2001**, *124*, 318–326.
- (23) Kalé, L.; Skeel, R.; Bhandarkar, M.; Brunner, R.; Gursoy, A.; Krawetz, N.; Phillips, J.; Shinozaki, A.; Varadarajan, K.; Schulten, K. *J. Comput. Phys.* **1999**, *151*, 283–312.
- (24) Humphrey, W.; Dalke, A.; Schulten, K. *J. Mol. Graphics* **1996**, *14*, 33–38.
- (25) Lindahl, E.; Edholm, O. *J. Chem. Phys.* **2000**, *113*, 3882–3893.
- (26) Gullingsrud, J.; Schulten, K. *Biophys. J.* **2004**, *86*, 3496–3509.
- (27) One can prepare a system of randomly distributed oleic acid molecules in water and then relax to see if the triple-structure can be obtained. For this system, however, the ratios of oleic acid to water molecules are unknown. Therefore, one reliable setup, as we used, is to start from a well-known crystalline structure.
- (28) Budin, I.; Szostak, J. W. *Proc. Natl. Acad. Sci. U.S.A.* **2011**, *108*, 5249–5254.
- (29) We performed test simulations on the force-field parameters of oleic acid by computing elastic moduli of an orthorhombic crystal in the γ -phase. The bulk modulus is 1.86 GPa . The Young's moduli are $E_{xx} = 3.5\text{ GPa}$, $E_{yy} = 0.9\text{ GPa}$, and $E_{zz} = 0.9$. E_{xx} is the greatest because the hydrocarbon chains align in the x -direction. These values agree with those of polystyrene and polyethylene (Ciprari, D.; Jacob, K;

- Tannenbaum, R. *Macromolecules* **2006**, *39*, 6565–6573; Klapperich, C.; Komvopoulos, K.; Pruitt, L. *J. Tribol.* **2001**, *123*, 624–631), and the experimentally measured elastic modulus of oleic acid functionalizing lead sulfide nanoparticles (1.7 GPa) (Tam, E.; Podsiadlo, P.; Shevchenko, E.; Ogletree, D. F.; Delplancke-Ogletree, M.-P.; Ashby, P. D. *Nano Lett.* **2010**, *10*, 2363–2367).
- (30) Klauda, J. B.; Venable, R. M.; Freites, J. A.; O'Connor, J. W.; Tobias, D. J.; Mondragon-Ramirez, C.; Vorobyov, I.; MacKerell, A. D.; Pastor, R. W. *J. Phys. Chem. B* **2010**, *114*, 7830–7843.
- (31) Marrink, S.-J.; Berendsen, H. J. C. *J. Phys. Chem.* **1994**, *98*, 4155–4168.
- (32) Almeida, P. F. F.; Vaz, W. L. C.; Thompson, T. E. *Biochemistry* **1992**, *31*, 6739–6747.
- (33) Bearman, R. J.; Jolly, D. L. *Mol. Phys.* **1981**, *44*, 665–675.
- (34) Vanegas, J. M.; Longo, M. L.; Faller, R. *J. Am. Chem. Soc.* **2011**, *133*, 3720–3723.
- (35) Baoukina, S.; Monticelli, L.; Marrink, S. J.; Tielemans, D. P. *Langmuir* **2007**, *23*, 12617–12623.
- (36) Crane, J. M.; Putz, G.; Hall, S. B. *Biophys. J.* **1999**, *77*, 3134–3143.
- (37) Borgnia, M. J.; Agre, P. *Proc. Natl. Acad. Sci. U.S.A.* **2001**, *98*, 2888–2893.
- (38) Zeidel, M. L.; Ambudkar, S. V.; Smith, B. L.; Agre, P. *Biochemistry* **1992**, *31*, 7436–7440.
- (39) de Groot, B. L.; Grubmüller, H. *Science* **2001**, *294*, 2353–2357.
- (40) Gurtovenko, A. A.; Anwar, J.; Vattulainen, I. *Chem. Rev.* **2010**, *110*, 6077–6103.
- (41) Abrahamsson, S.; Ryderstedt-Nahringerbauer, I. *Acta Crystallogr.* **1962**, *15*, 1261–1268.
- (42) Chen, S.; Seidel, M. T.; Zewail, A. H. *Proc. Natl. Acad. Sci. U.S.A.* **2005**, *102*, 8854–8859.